



Shift in the percolation threshold of compressed composites —A 3D Monte Carlo simulation*

Chuan LIN¹, Hong-tao WANG², Wei YANG^{†‡1,2}

⁽¹⁾Applied Mechanics Laboratory, Department of Engineering Mechanics, Tsinghua University, Beijing 100084, China)

⁽²⁾Institute of Applied Mechanics, Zhejiang University, Hangzhou 310027, China)

[†]E-mail: yangw@zju.edu.cn

Received May 1, 2010; Revision accepted July 30, 2010; Crosschecked Sept. 15, 2010

Abstract: The shift in the percolation threshold of compressed composites was studied by a 3D continuum percolation model. A Monte Carlo (MC) method was employed in the simulations. The percolation threshold was found to rise with the compression strain, which captures the basic trend in compression-induced conductivity variation from the experiments. Both fiber bending and texture formation contribute to the percolation threshold. The results suggest that fillers with a high aspect ratio are more desirable for sensor and electrical switch applications.

Key words: Monte Carlo (MC) model, Percolation threshold, Compressed composites

doi:10.1631/jzus.A1000207

Document code: A

CLC number: TB303

1 Introduction

Both scientific and technological communities are impressed with the piezoresistive effect of polymer-based nanocomposites (Carmona *et al.*, 1987; Zhang *et al.*, 2000; Hussain *et al.*, 2001; Dang *et al.*, 2007). The scientific interest is caused by the creation of piezoresistance from two non-piezoresistive components, while the technological advantage lies in the low processing cost of polymers. The root of this effect can be traced to the percolation theory, which leads to a general formulation in the form of $\sigma \propto (\phi - \phi_c)^t$, where σ is the conductivity, t the critical exponent, ϕ the volume fraction, and ϕ_c the percolation threshold (Kirkpatrick, 1973). When ϕ is close to ϕ_c , a sharp conductivity change is expected for even a

slight variation of ϕ (or ϕ_c), by deforming the composites. Early experiments demonstrated that the hydrostatic pressure led to the increase of conductivity in four polymer-matrix composites that filled with carbon particles (Carmona *et al.*, 1987; Wichmann *et al.*, 2009). A phenomenological theory that accounted for the pressure-induced volume fraction increase was developed to correlate the experimental data (Carmona *et al.*, 1987). Piezoresistance effect has also been found in composites with rubber matrix under uniaxial compression (Zhang *et al.*, 2000). Subjected to compression, the nearly incompressible feature of the rubbers inevitably shortens the distances among rigid carbon particles. Consequently, more conducting paths may be formed to align with the compression direction and the percolation threshold is lowered.

For composites with conducting fibers, however, the above trend in the piezoresistance effect may be reversed. The composites with conducting fibers are more of application interest due to the extremely low percolation threshold (<1%) (Li and Chou, 2007; Bauhofer and Kovacs, 2009; Ma *et al.*, 2010), com-

[‡] Corresponding author

* Project supported by the National Natural Science Foundation of China (No. 10832009), the National Basic Research Program (973) of China (No. 2004CB619304), and the Science Foundation of Chinese University (No. 2009QNA4034)

© Zhejiang University and Springer-Verlag Berlin Heidelberg 2010

pared to that of the composites with particle fillers (–30%) (Safran *et al.*, 1985). To elucidate the underlying mechanisms, a 2D Monte Carlo (MC) model has been proposed by Lin *et al.* (2010). In the present work, we extend the MC simulation to 3D systems.

2 Simulation methods

An $L \times L \times L$ cubic matrix with fibers of unit length is chosen as the initial percolating system for MC simulations. The fiber is represented by an arc of radius R (Fig. 1) with an assumed circular cross-section of radius a . The aspect ratio (AR) is thus conveniently defined as $1/(2a)$. The fiber orientation is characterized by the two angles θ_i and ϕ_i . The center is located by the chord middle-point coordinates $M_i(X_i, Y_i, Z_i)$. To accelerate the contact points searching process, each fiber, e.g., the i th one, is uniformly discretized into $n+1$ points denoted as A_{i1} to A_{in+1} , and the adjacent points define n segments denoted as L_{i1} to L_{in} . An arm-shaped model has been used to study the electrical conductivity of polymer-based composites with curved fibers, which is equivalent in setting $n=2$ (Ma and Gao, 2008). To catch the details of deformation-induced bending, we take $n=10$ in this work. The i th and j th fibers are in contact only if $\min\{\text{distance}(L_{ik}, L_{jl}), k, l=1, 2, \dots, n\} \leq 2a$. The MC algorithm can be sketched by the following five steps: (1) add the i th fiber to the matrix according to randomly generated (X_i, Y_i, Z_i) , θ_i , and ϕ_i ; (2) search for contacts between the i th fiber and the fibers whose chord centers are within the cube defined by $|X-X_i| < 1$, $|Y-Y_i| < 1$, and $|Z-Z_i| < 1$; (3) assign a common cluster number for the connected fibers so that different clusters have different numbers; (4) merge two clusters (assigning both the smaller cluster number) when they are bridged by the i th fiber; and, (5) repeat step (1) to step (4) until the first percolating cluster was formed. The critical volume fraction ϕ_c was then determined by $n_c \pi a^2 / L^3$ with n_c being the critical number. The computation cost increases enormously with the matrix size and the discrete point number n of each fiber. To reduce the computer time to an affordable level, we take $L=10$ and $n=10$ for all simulations. The code was tested by calculating the percolation threshold for a composite sample with straight-fillers. The filler AR is taken to be 50. The probability density of

ϕ_c was obtained by repeating the MC simulations one hundred times and was fitted by a normal distribution (Fig. 2), as suggested by Li and Chou (2007). The mean value gives the percolation threshold $\phi_c = (1.30 \pm 0.03)\%$, which is in agreement with the result ($\phi_c = 1.3\%$) of Foygel *et al.* (2005).

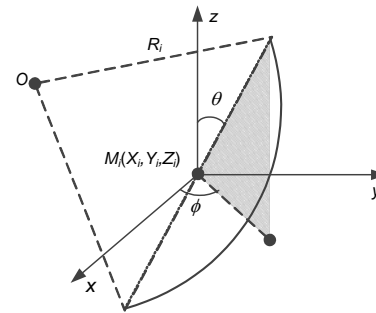


Fig. 1 Schematic representation of fiber fillers

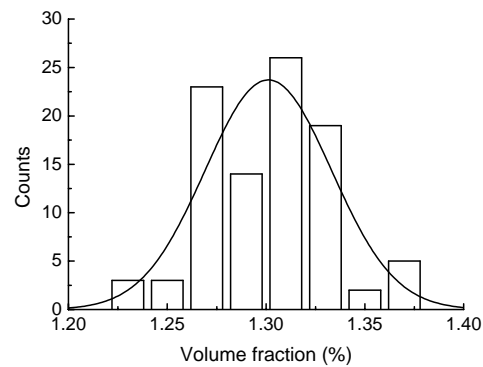


Fig. 2 Distribution of 100 MC simulations for a $10 \times 10 \times 10$ matrix (the percolation threshold ϕ_c is obtained by fitting)

3 Deformation effect

The polymer matrix is generally much more compliant than the conducting fiber fillers, such as carbon nanotubes (CNTs). The latter possess high ARs and extraordinary mechanical and electrical properties (Yang *et al.*, 2008; Bauhofer and Kovacs, 2009). The embedded fiber retains its length under tension, but bends under compression. The bending effect of an initially straight fiber is modeled in the following two-step process. Firstly, the fiber is assumed to deform with the matrix. Assuming the matrix is incompressible, the coordinates before and after deformation transform are given below:

$$X = \frac{X^0}{\sqrt{1-\gamma}}, \quad Y = \frac{Y^0}{\sqrt{1-\gamma}}, \quad Z = Z^0(1-\gamma), \quad (1)$$

$\theta_i^0 > \theta_\lambda$ with

$$\theta_\lambda = \arctan \sqrt{(1-\gamma)(2-\gamma)}. \quad (2)$$

where the superscript “0” indicates the initial configuration and γ is the compression strain. Secondly, the deformed fiber length l is calculated in accordance to the given deformation mode:

$$l = \sqrt{\frac{\sin^2 \theta_i^0}{1-\gamma} + \cos^2 \theta_i^0 (1-\gamma)^2}, \quad (2)$$

with θ_i^0 being the polar angle of the initial straight fiber. If $l < 1$, it is replaced by an arc with the same ends and the unit length, as shown in Fig. 3a. The point $M(X_i, Y_i, Z_i)$ now becomes the middle point of the chord. The bending direction, i.e., the angle ϕ_i , is randomly given. Substituting $l < 1$ into Eq. (2), the following inequality is found to be satisfied when

Fig. 3b shows the “elongated fiber” when $l > 1$, as indicated by the dashed line. The angles θ_i and ϕ_i are kept and the two ends are relocated so as $|M_i A_{i1}| = |M_i A_{i2}| = 1/2$. The polar angle θ_λ is plotted in Fig. 3c for the incompressible matrix. The angle decreases with strain and is in the range of 26° – 45° for a compression strain up to 30%. The deformation mode depicted in Fig. 3 is suitable for describing the behaviors of composite with a compliant matrix, such as the widely-used rubbers, with fillers of high AR. Fig. 4a shows the initial configuration of a $10 \times 10 \times 10$ matrix with 200 straight fibers. After a compression strain of 30%, the deformed configuration is shown in Fig. 4b. The figure shows the change in connectivity, and thus the percolation threshold.

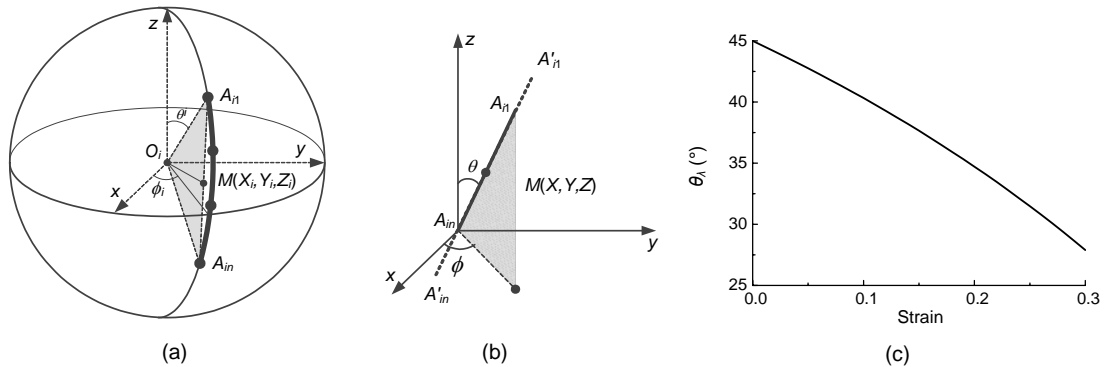


Fig. 3 Fiber geometry under local compression (a); Fiber geometry under local tension (b); Variation of θ_λ with strain (c)

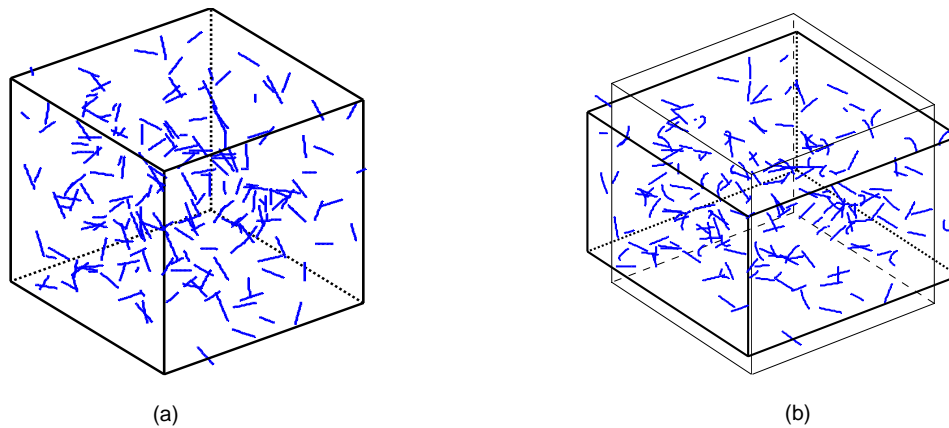


Fig. 4 Example of a 3D matrix ($10 \times 10 \times 10$) containing 200 fibers (a) before and (b) after compression

4 Results and discussion

The percolation behavior along the compression direction is focused. The percolation threshold increases with compression, in agreement with the observed decrease of conductivity in CNT-filled composites. The conductivity correlates to the density of the conducting paths. As predicted by the percolation theory, the formation of the conducting paths strongly depends on the difference between the volume fraction and the percolation threshold of the conducting fillers. For the rubber-like matrix, the bulk is isochoric under compression. Accordingly, the decrease in conductivity comes from the shift in the percolation threshold. This is confirmed by the MC simulations of a compressed composite with fiber AR=50 (Fig. 5). For 30% compression strain, the percolation threshold increases about 3.6%. The composite conductivity can be calculated from the universal power law:

$$\frac{\sigma}{\sigma_f} = \left(\frac{\phi - \phi_c}{1 - \phi_c} \right)^t, \text{ when } \sigma_f \gg \sigma_m, \quad (3)$$

where σ_f and σ_m denote the conductivities of the filler and the matrix, respectively. The critical exponent t is taken to be 2.5, according to the conductivity measurements for CNT-filled composites. Fig. 6 plots the compression-induced conductivity variation for different filler volume fractions. The conductivity remains nearly constant at compression strains less than 15%, then it down-slides at strains larger than 15% and loadings close to the percolation threshold. The insensitivity at small strains is due to the relatively small AR comparing to the real fiber-like fillers. For CNTs, the diameter is about 10 nm and the length is in the micrometer range, giving the AR>1000. For these ultra slim fillers, the bending effect is more pronounced under compression. Presumably, the percolation threshold would then increase with strain and the plateau region would vanish. On the other hand, for particle-filled composites, i.e., the limiting case with AR=-1, the percolation threshold decreases under compression.

Besides the fiber bending, deformation also assists fiber alignment. The fiber polar angles before and after the deformation are related by

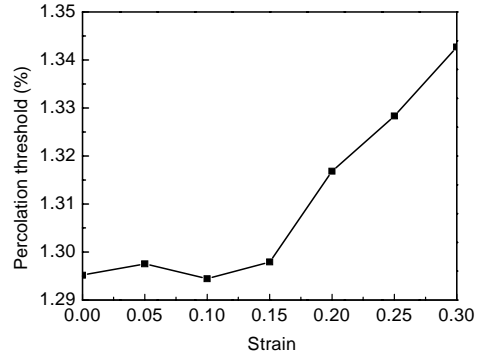


Fig. 5 Percolation thresholds versus compression strain for composites with an aspect ratio of fibers being 50 and a Poisson's ratio of the matrix being 0.5

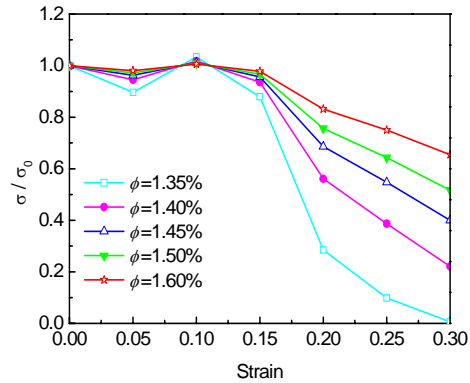


Fig. 6 Relative conductivity versus compression strain for different filler volume fractions

$$\theta = \arctan\left(\frac{1}{c} \tan \theta^0\right), \quad \phi = \phi^0, \quad (4)$$

where $c=(1-\gamma)^{3/2}$. The initial orientation is assumed to be fully random; i.e., $f_0(\theta^0, \phi^0) = \frac{\sin \theta^0}{2\pi}$ for $0 \leq \theta^0 \leq \pi/2$, $0 \leq \phi^0 \leq 2\pi$. After deformation, the probability density function becomes

$$f(\theta_i, \phi_i) = \frac{c^2}{2\pi} \sin(\arctan(c \tan \theta_i)) \frac{1 + \tan^2 \theta_i}{1 + c^2 \tan^2 \theta_i}. \quad (5)$$

Fig. 7 shows the distributions of orientation angles before and after compression. Please note that neither bending nor alignment plays a role in the particle-filled composite. The feature of orientation change in fiber-filled composites dictates its opposite behavior in piezoresistance from the particle-filled composites.

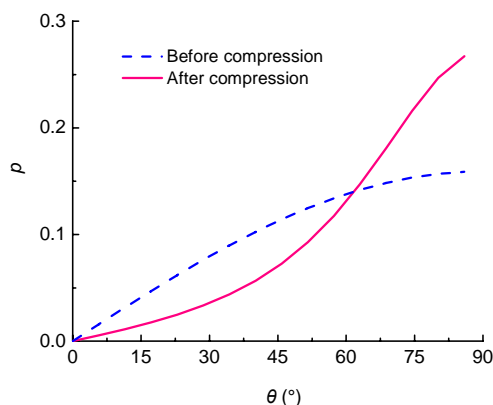


Fig. 7 Distribution of fiber orientations before and after compression of 30%

5 Conclusions

The piezoresistance effect in fiber-filled composites has been studied by 3D MC simulations. Though the fiber is simply modeled as an arc after bending, the simulation captures the general trend in compression-induced conductivity, similar to that from the experiments. For sensor and electrical switch applications, the high AR fillers are more desirable.

References

- Bauhofer, W., Kovacs, J.Z., 2009. A review and analysis of electrical percolation in carbon nanotube polymer composites. *Composites Science and Technology*, **69**(10): 1486-1498. [doi:10.1016/j.compscitech.2008.06.018]
- Carmona, F., Canet, R., Delhaes, P., 1987. Piezoresistance of heterogeneous solids. *Journal of Applied Physics*, **61**(7): 2550-2557. [doi:10.1063/1.337932]
- Dang, Z.M., Wang, L., Yin, Y., Zhang, Q., Lei, Q.Q., 2007. Giant dielectric permittivities in functionalized carbon-nanotube/electroactive-polymer nanocomposites. *Advanced Materials*, **19**(6):852-857. [doi:10.1002/adma.200600703]
- Foygel, M., Morris, R.D., Anez, D., French, S., Sobolev, V.L., 2005. Theoretical and computational studies of carbon nanotube composites and suspensions: Electrical and thermal conductivity. *Physical Review B*, **71**(10):104201. [doi:10.1103/PhysRevB.71.104201]
- Hussain, M., Choa, Y.H., Niihara, K., 2001. Fabrication process and electrical behavior of novel pressure-sensitive composites. *Composites Part A: Applied Science and Manufacturing*, **32**(12):1689-1696. [doi:10.1016/S1359-835X(01)00035-5]
- Kirkpatrick, S., 1973. Percolation and conduction. *Reviews of Modern Physics*, **45**(4):574-588 [doi:10.1103/RevModPhys.45.574]
- Li, C., Chou, T.W., 2007. Continuum percolation of nanocomposites with fillers of arbitrary shapes. *Applied Physics Letters*, **90**(17):174108. [doi:10.1063/1.2732201]
- Lin, C., Wang, H., Yang, W., 2010. Variable percolation threshold of composites with fiber fillers under compression. *Journal of Applied Physics*, **108**(1):013509. [doi:10.1063/1.3457351]
- Ma, H.M., Gao, X.L., 2008. A three-dimensional Monte Carlo model for electrically conductive polymer matrix composites filled with curved fibers. *Polymer*, **49**(19):4230-4238. [doi:10.1016/j.polymer.2008.07.034]
- Ma, H.M., Gao, X.L., Tolle, T.B., 2010. Monte Carlo modeling of the fiber curliness effect on percolation of conductive composites. *Applied Physics Letters*, **96**(6): 061910. [doi:10.1063/1.3309590]
- Safran, S.A., Webman, I., Grest, G.S., 1985. Percolation in interacting colloids. *Physical Review A*, **32**(1):506-511 [doi:10.1103/PhysRevA.32.506]
- Wichmann, M.H.G., Buschhorn, S.T., Gehrman, J., Schulte, K., 2009. Piezoresistive response of epoxy composites with carbon nanoparticles under tensile load. *Physical Review B*, **80**(24):245437. [doi:10.1103/PhysRevB.80.245437]
- Yang, J.H., Xu, T., Lu, A., Zhang, Q., Fu, Q., 2008. Electrical properties of poly(phenylene sulfide)/multiwalled carbon nanotube composites prepared by simple mixing and compression. *Journal of Applied Polymer Science*, **109**(2): 720-726. [doi:10.1002/app.28098]
- Zhang, X.W., Pan, Y., Zheng, Q., Yi, X.S., 2000. Time dependence of piezoresistance for the conductor filled polymer composites. *Journal of Polymer Science Part B Polymer Physics*, **38**(21):2739-2749. [doi:10.1002/1099-0488(20001101)38:21]